Thermodynamic Comparison of the Salt Dependence of Natural RNA Hairpins and RNA Hairpins with Non-Nucleotide Spacers†

D. Jeremy Williams and Kathleen B. Hall*

Department of Biochemistry and Molecular Biophysics, Washington University School of Medicine, St. Louis, Missouri 63110

Received July 8, 1996; Revised Manuscript Received September 24, 1996⊗

ABSTRACT: RNA hairpins with loops of either ten or eight nucleotides, or seven nucleotides with (ethylene glycol)$_n$ spacers, have been compared in experiments that measure the NaCl dependence of their thermodynamic properties. In 1 M NaCl, the eight-nucleotide RNA hairpin/loop has the most favorable folding free energy ($\Delta G^\circ = -8.6$ kcal/mol), while the RNAs containing the spacers are considerably more unstable ($\Delta G^\circ = -5.2$ to -5.7 kcal/mol); for these RNA/linker species, there are compensating reductions in favorable entropy and unfavorable enthalpy of the helix−coil transition. Preferential interaction coefficients ($\Delta\Gamma_N$) determined from analyses of melting transitions as a function of NaCl concentration are compared to determine the effect of the ethylene glycol on differential ion association. While the difference in ion association to the helix and coil states of the fully RNA molecules follows prediction, the RNAs with linkers do not, indicating that the description of their native and/or denatured state has changed.

The availability of an increasing variety of modified nucleotides and non-nucleotide substituents for incorporation into oligonucleotides has provided new methods for testing biological functions of nucleic acids. For example, poly(ethylene glycol) has been used in hammerhead ribozymes to successfully replace one of the arms (Fu et al., 1994); as the terminal loop in the TAR RNA hairpin, where stabilities of several linkers were compared (Ma et al., 1993); in substrates for a DNA helicase (Amaratunga & Lohman, 1993); in an RNA loop as a flexible tether (Williams & Hall, 1996); and in a pre-mRNA splicing substrate (Pasman & Garcia-Blanco, 1996). However, there have been few investigations to determine the physicochemical consequences for the structural and thermodynamic properties of nucleic acids containing these linkers. One example is that of Durand et al. (1990), describing solution properties of a DNA hairpin containing a hexa(ethylene glycol) loop, while Altmann et al. (1995) structurally characterize a similar DNA hairpin by NMR, concluding that the stem retains its normal B-form structure. However, more detailed experiments are necessary to understand how these linkers influence the stability and structure of the flanking nucleic acid.

Non-nucleotide spacers can also be used to determine the extent to which the overall and/or local counterion distribution is determined by the sequence, base, or sugar substituents and the number and spatial orientation of charged phosphate groups. For example, Record and co-workers have shown that, for a short oligomer, the dependence of the observed equilibrium constant of the helix−coil transition (K_{obs}) on uniunivalent salt activity ($a_\pm$) is a sensitive function of its length [equivalently the number of charged groups (N) on the oligomer] (Record & Lohman, 1978; Record et al., 1978; Olmsted et al., 1989, 1991). Since the value of $\partial(\log K_{obs})/\partial(\log a_\pm)$ is related directly to the difference in the degree of thermodynamic association of ions with the coil and helix species, respectively, it must follow that the degree of association of ions with an oligomer is a sensitive function of length. The degree of counterion association with short nucleic acids should be altered by the presence of the linker; in addition to providing fundamental data on nucleic acid properties, experiments of this sort are important for subsequent use of these non-nucleotide spacers in biological contexts, such as protein binding.

The oligonucleotides examined in this work are RNA hairpins with a conserved heptanucleotide sequence (AUUGCAC) on the 5′ side of loops closed by CG base pairs (see Figure 1). The 3′ side of the loops contains either one or three nucleotides or poly(ethylene glycol) linkers [$(CH_2CH_2O)_{3,6,12}$]. Most of these hairpins are recognized by the human U1A protein (Williams & Hall, 1996), indicating that the linkers do not perturb the nucleotide environment in such a way as to block protein binding. However, those experiments did not directly examine the properties of the isolated RNA/linker hairpin. A detailed analysis of the enthalpic and entropic changes associated with the helix−coil transition of the different RNAs with and without ethylene glycol, and the salt dependence of the hairpin stability, is necessary to determine how these non-nucleotide linkers alter the solution properties of the RNA molecule. Here we report the results of a thermodynamic study of the sodium chloride dependence of the equilibrium constant (K_{obs}) and the melting temperature (T_M) of RNA hairpins with a ten-nucleotide loop (L10), an eight-nucleotide loop (L8), and three RNAs with linkers of three ($^1/_2$XL), six (1XL), or twelve (2XL) ethylene glycol units. The results are compared with previous theoretical and experimental studies of hairpin and duplex systems.

MATERIALS AND METHODS

RNA Synthesis and Purification. Oligonucleotides were synthesized enzymatically by SP6 RNA polymerase from DNA oligonucleotides as described (Stump & Hall, 1993) or chemically, using phosphoramidites and spacers (Spacer

† This work is supported in part by the Lucille P. Markey Charitable Trust (#90-47) and the NIH (GM46318).

* Correspondence should be addressed to this author. Phone: (314) 362-4196. Fax: (314) 362-7183. E-mail: hall@bionmr3.wustl.edu.

⊗ Abstract published in *Advance ACS Abstracts,* November 1, 1996.

S0006-2960(96)01654-6 CCC: $12.00

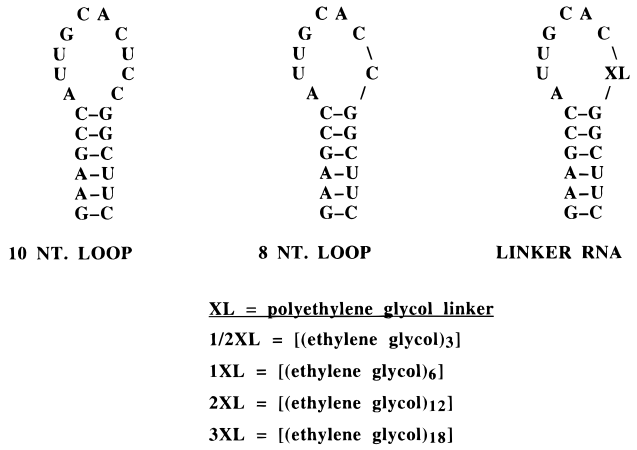

FIGURE 1: Sequences and assumed secondary structures of the RNA hairpins studied.

9 or Spacer 18) from Glen Research (Sterling, VA) and purified as described (Hall, 1994), except that a Dionex anion exchange column was used for HPLC purification. RNAs were dialyzed exhaustively against deionized distilled H_2O prior to use. Extinction coefficients of RNA molecules were calculated as described previously (Freier et al., 1983; Richards, 1975). RNAs synthesized by *in vitro* transcription begin with a 5′-pppG, while the chemically synthesized molecules have a 5′-hydroxyl.

Melting Curves. The buffer for thermodynamic studies was 10 mM sodium cacodylate and 0.5 mM Na_3EDTA at pH 7, to which specific amounts of NaCl were added. Thermodynamic stability of the various RNA hairpins was determined from the thermal denaturation of the purified RNA in a Gilford 260 spectrophotometer equipped with a 2527 Gilford thermoprogrammer. Absorbance measurements were taken at 260 nm with a heating rate of 1 °C/min. Samples were heated to 95 °C for 5 min immediately prior to starting melts and then were cooled slowly to 5 °C. Strand concentrations were determined at 95 °C from upper baselines. The RNA hairpins were melted over a 30−40-fold concentration range with no detectable variation in the melting temperature.

Data Analysis. Melting curves were fit using NONLIN (Johnson & Frasier, 1985) to a single intramolecular transition using the sloping baseline method (Freier et al., 1983). Convergence was set to 10^{-6} and parameter confidence intervals were estimated at 95%. The melting temperatures, equilibrium constants, and free energies were calculated from the corresponding van't Hoff $\Delta H°$ and $\Delta S°$ values, using the relation

$$K = \frac{\alpha}{(1-\alpha)} = \exp(-\Delta H°/RT + \Delta S°/R)$$

where α is the fraction of strands in the hairpin state, R the gas constant, and T the temperature in Kelvin (Freier et al., 1983), determined by global nonlinear regression of at least three independent experiments. Error propagation to calculate confidence intervals for the derived parameters was also done using NONLIN. Theoretical thermodynamic values for the all-RNA hairpins at 1 M salt were predicted using the MFOLD program (Zuker, 1994). For the salt dependence studies, equilibrium constants were calculated at an intermediate temperature in order to minimize extrapolation-related errors (65 °C for the $^1/_2$XL, 1XL, and 2XL hairpins; 70 °C for L8 and L10 RNA molecules). Total Na^+ concentrations were calculated from the sum of the NaCl and sodium cacodylate concentrations and then converted to molalities. The mean ionic activity ($a_\pm$) at a given temperature and molality was obtained by two-dimensional interpolation of the NaCl activity coefficients of Robinson and Stokes (1965) as a function of molality and temperature. The data were fit to straight lines using NONLIN with the convergence set to 10^{-6} and the confidence intervals determined at 95%.

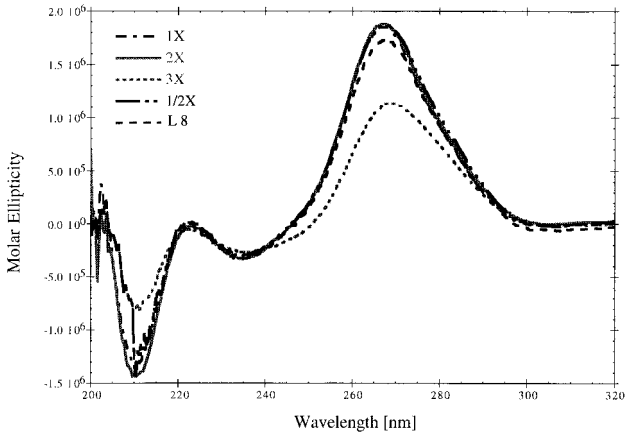

FIGURE 2: Circular dichroism spectra of five RNA substrates with 50 mM NaCl and 10 mM sodium cacodylate at pH 7 and 25 °C. Molar ellipticity is normalized to strand concentration.

Circular Dichroism Spectra. For the circular dichroism studies, the oligonucleotides were dissolved in 50 mM NaCl and 10 mM sodium cacodylate at pH 7. Spectra were recorded from 200 to 320 nm on a JASCO J600 spectropolarimeter at 23 °C; the molar ellipticity is normalized to the strand concentration.

RESULTS

RNA and RNA/Ethylene Glycol Structure. The circular dichroism spectra of the RNA hairpins were measured to compare the RNA with and without the linkers. All spectra (Figure 2) show classic A-form features, three of which, the $^1/_2$XL RNA/(ethylene glycol)$_3$, 1XL RNA/(ethylene glycol)$_6$, and 2XL RNA/(ethylene glycol)$_{12}$, are virtually indistinguishable. The ten-nucleotide loop RNA (L10) A-type spectrum (data not shown) is superimposable, suggesting that the substitution of ethylene glycol linkers for the three loop nucleotides does not significantly perturb the RNA structure in the stem or loop of the hairpin (as monitored by circular dichroism). The spectrum of the L8 hairpin shows a relatively reduced molar ellipticity maximum but is otherwise very similar over the wavelength range examined (205−320 nm). The 3XL (ethylene glycol)$_{18}$/RNA spectrum shows significant deviations from the other four, of which the most striking features are the reduced extrema at 265, 230, and 210 nm and a red shift of its crossover point. It is therefore likely that the overall structure is perturbed significantly by the introduction of this long spacer. The 3XL hairpin is not considered further in this study, but preliminary measurements indicate that its solution properties will be interesting to investigate further.

Consistent with hairpin (stem−loop) geometries, the five RNA constructs all exhibit unimolecular (i.e., concentration independent) helix−coil transitions as a function of temperature. Melting transitions were followed by monitoring the absorbance at a wavelength of 260 nm. Individual spectra show species specific characteristics, although overall, the

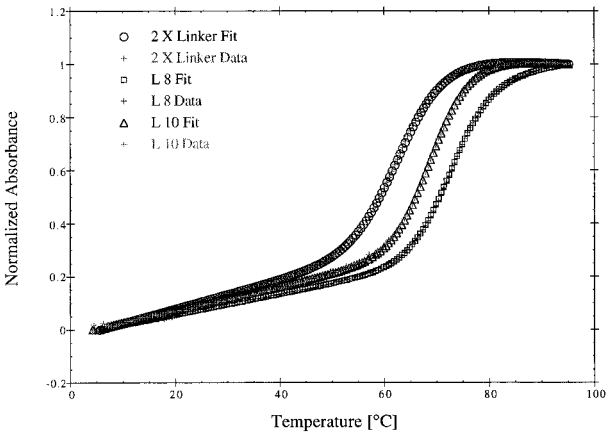

FIGURE 3: Normalized absorbance at 260 nm vs temperature for three RNA hairpins with fits to a two-state model with sloping baselines superimposed. Experimental conditions: 50 mM NaCl, 0.5 mM EDTA, 10 mM sodium cacodylate, and pH 7. Baselines were floated in the fitting routines.

spectra are quite similar to each other (see Figure 3 for representative spectra). The L10 and L8 isotherms show somewhat steeper transition regions than the corresponding linker transitions, suggesting a higher degree of cooperativity for the helix−coil transitions of the all-RNA hairpins. Calorimetric determination of the cooperative (melting) unit sizes for these hairpins will be necessary to properly address this issue. However, for the purpose of this study, it has been assumed that the five RNA hairpins have cooperative units with similar sizes.

Predictions of hairpin stability for the RNAs were based on the nearest neighbor model (Turner et al., 1988; Zuker, 1994), using parameters determined from oligonucleotide studies in 1 M NaCl. Table 1 lists experimental values of thermodynamic parameters for the five hairpins at the standard 1 M NaCl condition and the predicted values for the L10 and L8 hairpins. The theoretical prediction consistently underestimates the stability of these hairpins, although the stability difference between these hairpins is predicted to be a little over 2 °C, in perhaps fortuitous agreement with the experimental data. Agreement between the predicted and experimental free energies at 37 °C is less good, but this is not surprising in view of the very long extrapolation necessary to obtain the experimental values. There are no appropriate thermodynamic parameters for the RNA/ethylene glycol species.

Salt Dependence of Denaturation. In addition to the standard characterization of thermodynamic parameters in 1 M NaCl, the salt dependence of the melting transition of each hairpin was determined. Thermodynamic parameters were determined from the melting data at each salt concentration (Freier et al., 1983) from global fits of at least three independent experiments, as described previously. Parameters were derived by fitting the data to a two-state model with linear baselines; results are summarized in Table 2. The molecules can be divided into three classes on the basis of the magnitude of the $\Delta H°$ and $\Delta S°$ values: one containing the all-RNA molecules, a second composed of the $^1/_2$XL and 1XL hairpins, and a third, intermediate between these two, containing the 2XL hairpin. Within the scatter of the data, there is no significant dependence of the enthalpy or entropy on the sodium chloride concentration, although it is clear from Figures 4 and 5 that both the T_m and the K_{obs} show a power dependence on the mean sodium chloride activity; this trend should be reflected in either $\Delta H°$ or $\Delta S°$. However, it is difficult to accurately determine $\Delta H°$ and $\Delta S°$ simultaneously from a van't Hoff analysis. A typical correlation analysis of the fitted parameters using NONLIN (Johnson & Frasier, 1985) yields cross-correlation coefficients greater than 0.99 for the enthalpy and entropy. In addition, these two parameters are strongly correlated with the slopes and intercepts of the single strands (correlation coefficients > 0.6). Thus, caution must be exercised in interpreting small changes in either of these two parameters. However, the T_m and K_{obs} or $\Delta G°$ determined near the melting temperature are much more reliable. With these caveats in mind, it is nevertheless evident that the substitution of three nucleotides with ethylene glycol spacers decreases both the enthalpic cost and the favorable entropy change of unfolding. The changes in $\Delta H°$ and $\Delta S°$ are partially compensating, leading to an overall destabilization of only 0−6 °C depending on the salt concentration. Although one can speculate on the molecular origin of these differences, an *a priori* partitioning of the effect of the linker substitution between the helix and coil states is not possible.

The melting transitions for the five hairpins are also analyzed in terms of the T_M and the equilibrium constant (K_{obs}) as a function of the mean ion activity ($a_\pm$). These data are illustrated in Figures 4 and 5. Above 50 mM NaCl, stability trends as monitored by either the equilibrium constant or the melting temperature are identical. The molecules in decreasing order of stability are L8 > L10 > $^1/_2$XL > 1XL > 2XL. The observation that within a particular group (natural or linker RNAs) the stability decreases with larger loop size is consistent with the hypothesis that, as the number of loop nucleotides increases, the entropy of closing the loop becomes increasingly unfavorable.

However, a more general analysis of this nature is complicated by differences in the salt dependence of the hairpin stabilities. At the lowest salt concentration used (10 mM NaCl), the relative order of stabilities of the RNAs is apparently unpredictable, and the exact stability trend depends on whether one monitors the melting temperature [$\partial T_m/\partial(\ln a_\pm)$] or the equilibrium constant [$\partial(\ln K_{obs})/\partial(\ln a_\pm)$].

We note that the melting temperatures predicted at 1 M NaCl from extrapolation of the results of the salt dependence studies are invariably found to be 2−5 °C higher than the measured values at 1 M salt, suggesting a downward curvature of the slope of a $\ln K_{obs}$ vs $\ln a_\pm$ plot at higher salt. At salt concentrations approaching 1 M, anion or preferential hydration effects may not be insignificant and must be taken into account (Record et al., 1978). Although for polymers $\partial(\ln K_{obs})/\partial(\ln a_\pm)$ or $\partial T_m/\partial(\ln a_\pm)$ is relatively constant to 1 M salt, for short oligomers, there is no reason *a priori* to expect such linearity over such a wide salt concentration.

DISCUSSION

Hairpin Stability. Introduction of the ethylene glycol linkers into the loop region of the RNA hairpin has resulted in a destabilization of the hairpin at NaCl concentrations above 50 mM NaCl. Below this salt concentration, hairpin stability seems to correlate loosely with the size of the loop; the L8 RNA is the most stable, and the $^1/_2$XL is slightly more stable than the L10 RNA, on the basis of the melting temperature. The relative loop size in this comparison is based on the maximum extended length of the inserted linker,

Table 1: Standard State Thermodynamic Parameters[a]

	experimental data				predicted values			
	$\Delta H°$ (kcal/mol)	$\Delta S°$ (eu)	T_M (°C)	$\Delta G°_{37}$ (kcal/mol)	$\Delta H°$ (kcal/mol)	$\Delta S°$ (eu)	T_M (°C)	$\Delta G°_{37}$ (kcal/mol)
L10	67.4 (±4%)	189.5 (±4%)	82.4 (0.5−1.0)	8.6 (±3%)	63.4 (±10%)	181.0 (±11%)	77.3 (2−4)	7.3 (±5%)
L8[b]	62.0 (±6%)	173.1 (±6%)	84.7 (0.5−1.0)	8.3 (±5%)	63.4 (±10%)	179.7 (±11%)	79.9 (2−4)	7.7 (±5%)
2XL	49.3 (±4%)	141.70 (±4%)	74.6 (0.5−1.0)	5.3 (±3%)	–	–	–	–
1XL	47.8 (±4%)	137.3 (±5%)	75.2 (0.5−1.0)	5.2 (±4%)	–	–	–	–
$^1/_2$XL	50.2 (±7%)	143.6 (±8%)	76.7 (1.0−2.0)	5.7 (±6%)	–	–	–	–

[a] Conditions: 1 M NaCl, 0.5 mM Na_3EDTA, 10 mM sodium cacodylate, and pH 7. [b] Confidence intervals obtained with upper baselines fixed.

Table 2: Helix−Coil Thermodynamics[a]

	L10		L8		2XL		1XL		$^1/_2$XL	
[NaCl] (mM)	$\Delta H°$ (kcal/mol)	$\Delta S°$ (eu)	$\Delta H°$ (kcal/mol)	$\Delta S°$ (eu)	$\Delta H°$ (kcal/mol)	$\Delta S°$ (eu)	$\Delta H°$ (kcal/mol)	$\Delta S°$ (eu)	$\Delta H°$ (kcal/mol)	$\Delta S°$ (eu)
10	61.1	182.1	62.9	185.0	53.8	163.0	44.2	132.3	44.0	131.0
25	58.9	174.1	69.8	203.5	48.3	145. 2	50.8	150.7	44.8	132.8
50	62.5	182.4	60.4	174.5	50.1	148.8	45.9	135.0	42.3	124.2
100	63.8	184.3	66.8	191.5	58.6	172.6	45.5	133.4	55.7	162.8
200	62.3	178.1	66.3	188.5	47.8	139.4	47.7	13 8.6	43.5	125.9
1000[b]	67.4	189.5	62.0	173.1	49.3	141.7	47.8	137.3	50.2	143.6
min/max[c]	4.3/8.7	4.4/8.9	3.7/16.7	3.8/16.9	6.7/12.1	6.7/12.2	11.5/16.7	11.7/17.0	11.5/15.8	11.9/16.1
avg[c]	6.3	6.5	9.9	10.1	9.9	10.0	13.5	13.8	13.5	13.8

[a] Thermodynamic values are for helix to coil (melting) transitions. Conditions: 0.5 mM Na_3EDTA, 10 mM sodium cacodylate, and pH 7. [b] Data not used in salt dependence calculations. [c] Minimum, maximum, and average (percentage) width of confidence interval about the $\Delta H°$ or $\Delta S°$ values at the 95% confidence level (≈2 SD).

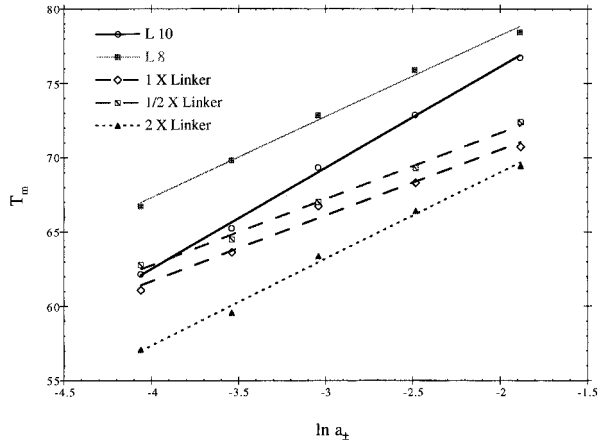

FIGURE 4: Variations of T_M as a function of salt concentration. Lines are linear least-squares fits to the data. NaCl concentration varied in a buffer containing 0.5 mM EDTA and 10 mM sodium cacodylate at pH 7. Melting temperatures calculated from corresponding $\Delta H°$ and $\Delta S°$ values determined from global nonlinear regression analysis of three or more independent experiments.

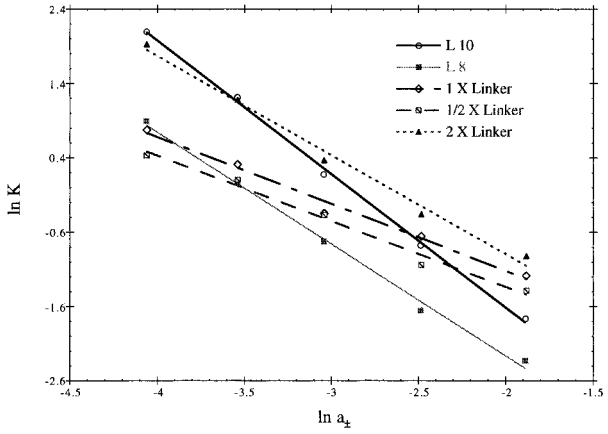

FIGURE 5: Variations of ln K_{obs} as a function of salt concentration. Lines are linear least-squares fits to the data. NaCl concentration varied in a buffer containing 0.5 mM EDTA and 10 mM sodium cacodylate at pH 7. Equilibrium constants calculated at 65 °C ($^1/_2$XL, 1XL, and 2XL) or 70 °C (L8 and L10 RNAs) from corresponding $\Delta H°$ and $\Delta S°$ values determined from global nonlinear regression analysis of three or more independent experiments.

which has been estimated for the $(ethylene\ glycol)_{3,6}$ by Monte Carlo/stochastic dynamic simulations (Williams & Hall, 1996). The $^1/_2$XL was shown by those simulations to be equivalent at full extension (span from 3.5 to 12.9 Å) to the O3′−O3′ span of two nucleotides (6.2−13.7 Å, measured from tRNA structures in the Brookhaven Protein Data Bank), while the 1XL is potentially longer than three nucleotides. By this estimation, the loop size of $^1/_2$XL RNA is equivalent to that of L8 RNA, while the 2XL RNA loop is larger than L10. However, it is unlikely that the linker is fully extended in these loops in solution; the root mean square value of the linker length, 8 and 9 Å for $^1/_2$XL and 1XL, respectively, is a more probable description of its average extension, given the flexibility of poly(ethylene glycol) and the seven nucleotides in the loop that can also exhibit conformational flexibility. In addition to changing the effective length of the loop, the linker insertions also alter the charge distribution, since the linkers are uncharged. The response of the hairpins to NaCl may reflect a difference in ion density around the RNA.

Table 3: Salt Dependence of Hairpin Denaturation[a]

	$-SK_{obs}$	$-IK_{obs}$	ST_M	IT_M	N[b]	$-\Delta\Gamma_N$[c]	$-\Delta\Gamma_N$[d]
L10	1.8	5.2	6.8	89.7	22−24	0.037−0.041	0.035−0.038
	(2.0−1.6)	(5.8−4.6)	(6.0−7.6)	(87.2−92.2)			
L8	1.5	5.3	5.4	89.1	20−22	0.034−0.038	0.031−0.035
	(1.8−1.3)	(6.1−4.5)	(4.5−6.4)	(86.1−92.1)			
2XL	1.3	3.6	5.8	80.6	20	0.035	0.031
	(1.7−1.0)	(4.6−2.5)	(4.7−6.9)	(77.3−84.0)			
1XL	0.9	2.9	4.4	79.4	19	0.024	0.028
	(1.2−0.6)	(3.8−2.1)	(3.0−5.8)	(75.0−83.7)			
$^1/_2$XL	0.9	3.1	4.5	80.5	19	0.023	0.028
	(1.2−0.6)	(3.9−2.3)	(3.7−5.3)	(78.1−83.0)			

[a] Slopes and intercepts from unweighted least-squares regression of ln K_{obs} and T_M vs ln $a_\pm$. Confidence intervals (95%) shown in parentheses. [b] Actual number of phosphates. Note that the all-RNA molecules have a 5′-pppG while the others have a 5′-OH. [c] Experimental value of preferential interaction coefficient normalized to the number of phosphates. [d] Predicted (theoretical) value of preferential interaction coefficient per phosphate.

Ion Binding. Record and co-workers have shown that one can relate the magnitude of the salt dependence to differences in the degree of thermodynamic association of ions with the helix and coil forms (Anderson & Record, 1982; Bond et al., 1994). On the basis of their formulation, one can write a general equation describing these salt effects:

$$\frac{\partial(\ln K_{obs})}{\partial(\ln a_\pm)} = -\frac{\Delta H^\circ}{RT_M{}^2}\frac{\partial T_M}{\partial(\ln a_\pm)} = 2N\Delta\Gamma_N$$

Here $\Delta\Gamma_N$ is the stoichiometrically weighted difference in preferential interaction coefficients (defined per monomer unit, or phosphate charge, N), and it is directly related to the slope of a plot of ln K_{obs} vs ln $a_\pm$, the uniunivalent mean ion activity. If the difference in degree of thermodynamic association of ions with the helix and coiled forms is independent of $a_\pm$, such a plot will be linear. If in addition the ratio of $\Delta H^\circ/RT_M{}^2$ is constant, then a plot of the melting temperature as a function of ln $a_\pm$ will also be linear. A necessary (although not sufficient) condition for trends in the two plots (T_m and ln K_{obs} vs ln $a_\pm$) to be equivalent is that the ratio $\Delta H^\circ/RT_M{}^2$ must be the same for each molecule being compared.

The T_M and ΔH° for each hairpin were determined from the fit of their denaturation curves at a given NaCl concentration (Table 2). This enthalpy is for the entire RNA molecule, not, as in some applications, the enthalpy per monomer (Olmsted et al., 1991); N is the number of phosphates, and the preferential interaction coefficient $\Delta\Gamma_N$ is per phosphate. The mean ion activity of the NaCl was determined as described. As shown in Figures 4 and 5, for the five hairpins studied, plots of ln K_{obs} vs ln $a_\pm$ and T_m vs ln $a_\pm$ are linear. From the slopes of these plots, $\Delta\Gamma_N$ can be calculated, knowing the number of phosphates in the RNA. These values are given in Table 3. Note that the uncertainty in N for the all-RNA molecules comes from the 5′-pppG, which is subject to hydrolysis.

The experimentally determined $\Delta\Gamma_N$ can be compared to the theoretical prediction based on a recent analysis (Olmsted et al., 1991) of earlier DNA hairpin data (Elson et al., 1970). The formalism of Olmsted et al. (1991) predicts the preferential interaction coefficient change for an oligomer of length N, from the value for the corresponding polymer ($\Delta\Gamma_\infty$) and an end effect parameter ΔD using the following relationship:

$$\Delta\Gamma_N = \Delta\Gamma_\infty - \Delta D/N$$

The applicability of this relation to short oligomers was illustrated for DNA hairpins, which give the experimental values of $\Delta\Gamma_\infty = -0.077$ and $\Delta D = -0.93$, with $\Delta\Gamma_N = -0.035 \pm 0.016$ ($N = 22$) in a NaCl range of 3−60 mM (Olmsted et al., 1991). Since this $\Delta\Gamma_N < 0$, there is a release of ions upon melting. For the L10 and L8 RNA hairpins, the experimental values of the preferential interaction coefficients are given in Table 3, where they are compared to the values calculated from the above relation (using the experimental values of $\Delta\Gamma_\infty$ and ΔD determined from the DNA hairpin data). The average experimental values of $\Delta\Gamma_N = -0.039$ and -0.036 ($N = 22-24$ and $20-22$) obtained for the L10 and L8 RNAs, respectively, are in agreement with the predicted $\Delta\Gamma_N$, which is rather surprising considering the size of the RNA loops. Although, in principle, fortuitous compensating effects cannot be ruled out, these results suggest that this formalism can accurately describe oligoelectrolyte effects.

The linker-containing hairpins present a somewhat more complicated situation for analysis. Plots of T_M or ln K_{obs} vs ln $a_\pm$ for the $^1/_2$XL and 1XL hairpins have slopes that are identical within experimental error. A comparison of the experimental $\Delta\Gamma_N$ of -0.024 with predicted values of $\Delta\Gamma_N$ (Table 3) reveals that the experimental values for these linkers are distinctly smaller. Using the experimentally determined value of $\Delta\Gamma_N$ and the theoretical parameters of $\Delta\Gamma_\infty$ and ΔD to determine N gives a value of 17−18 phosphates for these two species, which actually have 19 phosphates. In principle, one could rationalize these differences (if significant) as being due to a linker-induced perturbation of the loop structure that results in fewer ions bound. Alternatively, small differences in the size of the cooperative melting unit could be responsible for the small deviations. Whatever their origin, the apparent discrepancies for the 1XL and $^1/_2$XL molecules are small in magnitude.

The situation is reversed for the 2XL RNA, where experimentally $\Delta\Gamma_N = -0.035$, and a similar analysis gives an apparent N of 22 phosphates, compared to the 20 actually present. There is no evidence that aggregation is an important factor at these concentrations ([RNA] $\approx 2.5\ \mu$M), and a calculated value of N greater than the actual number of charges in the molecule cannot be attributed simply to a larger cooperative melting unit. The larger than expected slope could be due to increased ion association with the helix form, decreased ion association with the single-stranded form, or both. Increased stacking interactions in the loop of the 2XL RNA may change the local charge distribution and could conceivably result in a higher fraction of counterions being associated with the 2XL hairpin. The unfolding enthalpy of this molecule is slightly more favorable than that

of the other linker/RNA hairpins; if base stacking is the dominant contribution to this term, then this explanation may be valid.

One less obvious consequence of the spacer is that it divides the single-stranded species into two strands of unequal length (six and thirteen phosphates long). As a result of the long range nature of Coulombic forces, coiled species having sufficiently short lengths of abasic linker can be viewed as contiguous 19-phosphate single strands. However, with increasing lengths of the intervening linker, the two regions of the single-stranded form will increasingly adopt the oligoelectrolyte characteristics of the shorter isolated strands. Because the magnitude of the preferential interaction coefficient decreases with the decreasing number of phosphates, the degree of ion association with the single strand will decrease as the length of the intervening linker increases (Olmsted et al., 1989, 1991). A smaller degree of ion association with the single-stranded form of the 2XL molecule relative to the 1XL and $^1/_2$XL hairpins is therefore an equally likely contribution to its anomalous $\Delta\Gamma_N$.

In a series of elegant grand canonical Monte Carlo experiments, Record and colleagues (Olmsted et al., 1991) demonstrated that differences in the length dependence of Γ_N predicted by simulation could explain the puzzling differences in the magnitudes of $\Delta\Gamma_N$ for the denaturation of short duplexes and hairpins (Elson et al., 1970; Erie et al., 1987; Williams et al., 1989; Braunlin & Bloomfield, 1991). For a given length and sequence composition, a duplex dimer shows a much larger value of $\Delta\Gamma_N$ than the corresponding hairpin. This is a direct consequence of the number of phosphates per strand being halved upon denaturation of a duplex dimer, whereas the number of charged groups per strand remains constant for a unimolecular hairpin transition. Therefore, the coiled form of the duplex has a lower fraction of associated counterions than does the hairpin and a correspondingly larger fractional change upon denaturation. For these RNA/linker hairpins, we predict that the 3XL species may approach the duplex/single-strand limit; however, a comparison of the salt dependence of the helix−coil transition for a series of identical duplexes joined by variable lengths of a flexible abasic linker, such as the DNA/ethylene glycol system of Altmann et al. (1995), could be a simpler system to investigate these effects. The prediction is that the magnitude of $\Delta\Gamma_N$ will increase with increasing linker length from a hairpin-like value to one more characteristic of a duplex.

SUMMARY

Insertion of ethylene glycol spacers in a large RNA hairpin loop has reduced the thermodynamic stability of the hairpin duplex; as the ethylene glycol length increases, the hairpin becomes less stable. It is not clear, however, if this effect is due to a reduction in the stability of the hairpin or an increase in the stability of the single strand. The sodium chloride dependence of the RNA stability with and without the linkers was measured to determine the differential extent of counterion association to the hairpins vs single strands. Introduction of the linkers appears to change the counterion density around the RNA, although whether this reflects ions bound to the hairpin or to the single strand is not known. One surprising result is the agreement of the experimentally determined preferential interaction coefficient with the values determined previously for DNA hairpins. Since RNA structures often preferentially bind Mg^{2+} ions, these experiments should be repeated with $MgCl_2$ to quantitatively describe the association of this divalent species with the RNA.

ACKNOWLEDGMENT

We thank Professor Tim Lohman for his always stimulating discussion and comments and Professor Tom Record for the inspiration for these experiments. W. Tom Stump continues to provide excellent technical assistance.

REFERENCES

Altmann, S., Labhardt, A. M., Bur, D., Lehmann, C., Bannwarth, W., Billeter, M., Wuthrich, K., & Leupin,W. (1995) *Nucleic Acids Res. 23*, 4827−4835.

Amaratunga, M., & Lohman, T. M. (1993) *Biochemistry 32*, 6815−6820.

Anderson, C. F., & Record, M. T., Jr. (1982) *Annu. Rev. Phys. Chem. 33*, 191−222.

Bond, J. P., Anderson, C. F., & Record, M. T., Jr. (1994) *Biophys. J. 67*, 825−836.

Braunlin, W. H., & Bloomfield, V. A. (1991) *Biochemistry 30*, 754−758.

Durand, M., Chevrie, K., Chassignol, M., Thuong, N. T., & Maurizot, J. C. (1990) *Nucleic Acids Res. 18*, 6353−6359.

Elson, E. L., Scheffler, I. E., & Baldwin, R. L. (1970) *J. Mol. Biol. 54*, 401−415.

Erie, D., Sinha, N., Olsen, W., Jones, R., & Breslauer, K. (1987) *Biochemistry 26*, 7150−7159.

Freier, S. M., Albergo, D. D., & Turner, D. H. (1983) *Biopolymers 22*, 1107−1131.

Fu, D.-J., Benseler, F., & McLaughlin, L. W. (1994) *J. Am. Chem. Soc. 116*, 4591−4598.

Hall, K. B. (1994) *Biochemistry 33*, 10076−10088.

Johnson, M. L., & Frasier, S. G. (1985) *Methods Enzymol. 117*, 301−342.

Ma, M. Y. X., Reid, L. S., Climie, S. C., Lin, W. C., Kuperman, R., Sumner-Smith, M., & Barnett, R. W. (1993) *Biochemistry 32*, 1751−1758.

Olmsted, M. C., Anderson, C. F., & Record, M. T., Jr. (1989) *Proc. Natl. Acad. Sci. U.S.A. 86*, 7766−7770.

Olmsted, M. C., Anderson, C. F., & Record, M. T., Jr. (1991) *Biopolymers 31*, 1593−1604.

Pasman, Z., & Garcia-Blanco, M. (1996) *Nucleic Acids Res. 24*, 1638−1645.

Record, M. T., Jr., & Lohman, T. M. (1978) *Biopolymers 17*, 159−166.

Record, M. T., Jr., & Anderson, C. F. (1995) *Biophys. J. 68*, 786−794.

Record, M. T., Jr., Anderson, C. F., & Lohman, T. M. (1978) *Q. Rev. Biophys. 11*, 103−178.

Richards, E. G. (1975) in *Handbook of Biochemistry and Molecular Biology: Nucleic Acids* (Fasman, G. D., Ed.) 3rd ed., Vol. I, p 597, CRC Press, Cleveland, OH.

Robinson, R. A., & Stokes, R. H. (1965) in *Electrolyte Solutions*, 2nd ed., p 480, Butterworths, London.

Stump, W. T., & Hall, K. B. (1993) *Nucleic Acids Res. 21*, 5480−5484.

Turner, D. H., Sugimoto, N., & Freier, S. M. (1988) *Annu. Rev. Biochem. Biophys. Chem. 17*, 167−192.

Williams, A. P., Longfellow, C. E., Freier, S. M., Kierzek,R., & Turner, D. H. (1989) *Biochemistry 28*, 4283−4291.

Williams, D. J., & Hall, K. B. (1996) *J. Mol. Biol. 257*, 265−275.

Zuker, M. (1994) in *Methods in Molecular Biology: Computer Analysis of Sequence Data* (Griffin, A. M., & Griffin, H. G., Eds.) Vol. 25 (II), p 267, Humana Press Inc., Totowa, NJ.

BI961654G